



Geophysical Research Letters

RESEARCH LETTER

10.1002/2017GL074431

Key Points:

- The MARSIS radar sounder has detected subsurface echoes deep within the Meridiani Planum deposits
- The time delay between surface and subsurface echoes is consistent with deposits having a low bulk value of the real dielectric constant
- New compaction relationships for Mars indicate that a low dielectric constant can be accounted for without invoking pore-filling water ice

Supporting Information:

- Supporting Information S1

Correspondence to:

T. R. Watters,
watterst@si.edu

Citation:






Watters, T. R., C. J. Leuschen, B. A. Campbell, G. A. Morgan, A. Cicchetti, J. A. Grant, R. J. Phillips, and J. J. Plaut (2017), Radar sounder evidence of thick, porous sediments in Meridiani Planum and implications for ice-filled deposits on Mars, *Geophys. Res. Lett.*, 44, 9208–9215, doi:10.1002/2017GL074431.

Received 2 JUN 2017

Accepted 17 AUG 2017

Published online 19 SEP 2017

Radar sounder evidence of thick, porous sediments in Meridiani Planum and implications for ice-filled deposits on Mars

Thomas R. Watters¹ , Carl J. Leuschen², Bruce A. Campbell¹ , Gareth A. Morgan¹ ,
Andrea Cicchetti³ , John A. Grant¹ , Roger J. Phillips⁴, and Jeffrey J. Plaut⁵

¹Center for Earth and Planetary Studies, Smithsonian Institution, Washington, District of Columbia, USA, ²Center for Remote Sensing of Ice Sheets, University of Kansas, Lawrence, Kansas, USA, ³Infocom Department, La Sapienza University of Rome, Rome, Italy, ⁴Department of Earth and Planetary Sciences and McDonnell Center for the Space Sciences, Washington University, St. Louis, Missouri, USA, ⁵Jet Propulsion Laboratory, California Institute of Technology, Pasadena, California, USA

Abstract Meridiani Planum is one of the most intensely studied regions on Mars, yet little is known about the physical properties of the deposits below those examined by the Opportunity rover. We report the detection of subsurface echoes within the Meridiani Planum deposits from data obtained by the Mars Advanced Radar for Subsurface and Ionospheric Sounding (MARSIS) instrument. The delay time between the surface and subsurface returns is indicative of materials with a real dielectric constant of 3.6 ± 0.6 . The real dielectric constant is strongly modulated by bulk density. Newly derived compaction relationships for Mars indicate that the relatively low dielectric constant of the Meridiani Planum deposits is consistent with a thick layer of ice-free, porous, basaltic sand. The unique physiographic and hydrologic setting of Meridiani Planum may have provided an ideal sediment trap for eolian sands. The relatively low gravity and the cold, dry climate that has dominated Mars for billions of years may have allowed thick eolian sand deposits to remain porous and only weakly indurated. Minimally compacted sedimentary deposits may offer a possible explanation for other nonpolar region units with low apparent bulk dielectric constants.

Plain Language Summary In spite of being among the most intensely studied regions of Mars, little is known about the makeup of the Meridiani Planum deposits below those examined by the Opportunity rover. The MARSIS radar sounder has detected subsurface echoes in Meridiani Planum. MARSIS transmits low-frequency radio pulses that can penetrate into certain crustal materials and are reflected back by dielectric discontinuities related to physical or compositional changes. Subsurface reflectors that are significantly offset in time delay from surface returns are interpreted to be from the interface between the Meridiani Planum deposits and buried ancient cratered terrain. The time delay is consistent with a material having a relatively low dielectric constant. Deposits on Mars with low dielectric constants are generally interpreted to indicate the presence of substantial water ice. The dielectric constant is strongly influenced by bulk density, and a thick sedimentary deposit will undergo significant self-compaction without the presence of pore-filling ice, increasing in bulk density and dielectric constant. Newly derived compaction relationships for Mars indicate that the relatively low dielectric constant of the Meridiani Planum deposits is consistent with a thick sequence of ice-free, porous, eolian sand. Thus, low dielectric constants are possible in other nonpolar deposits without the presence of water ice.

1. Introduction

Orbital and in situ exploration of the sedimentary deposits at Meridiani Planum has yielded important information on the occurrence and history of Martian water and potential habitability [Squyres and Knoll, 2005]. Meridiani Planum, situated within the equatorial highlands of Mars (Figure 1), is remarkable for its hematite-bearing deposits [Christensen *et al.*, 2000] and hydrated sulfates and hydrated iron oxides [Hynek *et al.*, 2002; Arvidson *et al.*, 2003, 2005; Gendrin *et al.*, 2005; Griffes *et al.*, 2007] detected from orbit. The Mars Exploration Rover Opportunity revealed that the hematite-bearing plains (HBP) include a lag of basaltic sand containing sulfates and hematitic concretions, likely derived from erosion of underlying rocks [Squyres *et al.*, 2004]. These HBP surficial deposits, characterized by smooth plains with occasional dunes, cover weakly indurated sandstones and are relatively thin compared to the thicker, underlying friable layered deposits of the etched plains (EP).

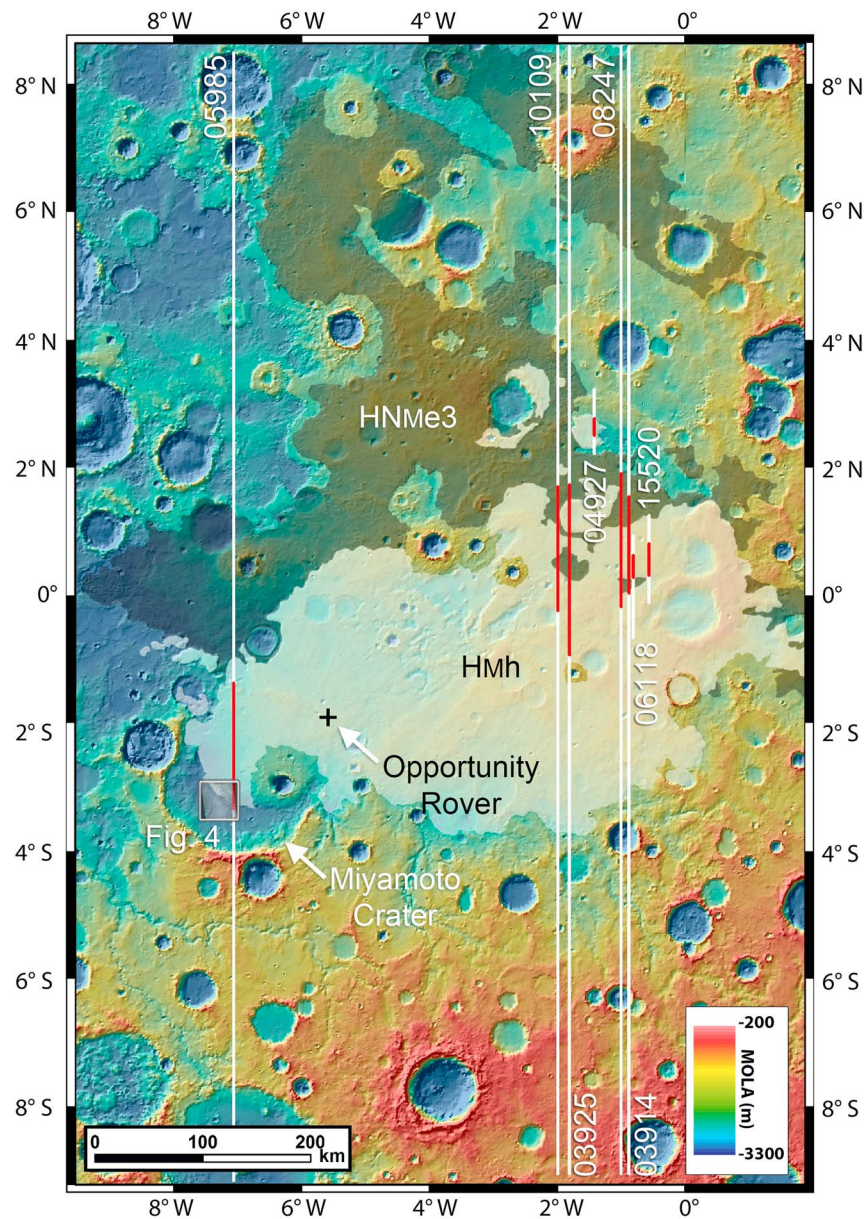


Figure 1. Mars Orbiter Laser Altimeter (MOLA) color-coded shaded relief of the Meridiani Planum region. The approximate locations of MARSIS SS3 mode orbit tracks 03914, 03925, 05985, 08247, and 10109 and the approximate locations of MARSIS Flash mode orbit tracks 04927, 06118, and 15520 are indicated by white lines. The approximate locations of the most prominent subsurface reflectors are shown by red line insets. The locations of subsurface reflectors are confined to geologic units HMh (transparent white—hematite unit, generally equivalent to HBP) and the underlying HNMe3 (transparent black—upper etched unit, generally equivalent to EP) mapped by Hynek and Di Achille [2017]. The location of the Opportunity rover is shown by the plus sign. Box shows the location of Figure 4.

The Mars Advanced Radar for Subsurface and Ionospheric Sounding (MARSIS) instrument on board the European Space Agency's Mars Express spacecraft operates in four frequency bands between 1.3 and 5.5 MHz [Picardi et al., 2005; Jordan et al., 2009; Orosei et al., 2015] and has been returning data since June 2005 (see supporting information Text S1). Two major units on Mars to date have been successfully probed: the polar layered deposits (PLD) [Plaut et al., 2007] and the Medusae Fossae Formation (MFF) [Watters et al., 2007], with the subsurface interface between these deposits and the underlying terrain clearly delineated. The MFF deposits occur at the equator along the Martian topographic dichotomy boundary and may be composed of volcanic ash, eolian sediments, or an ice-rich, layered material analogous to the PLD [Watters et al., 2007; Carter et al., 2009; Morgan et al., 2015]. The low attenuation of the radar pulses in the PLD is consistent with nearly pure water ice with only a few percent of admixed dust [Plaut et al., 2007; Phillips et al., 2008;

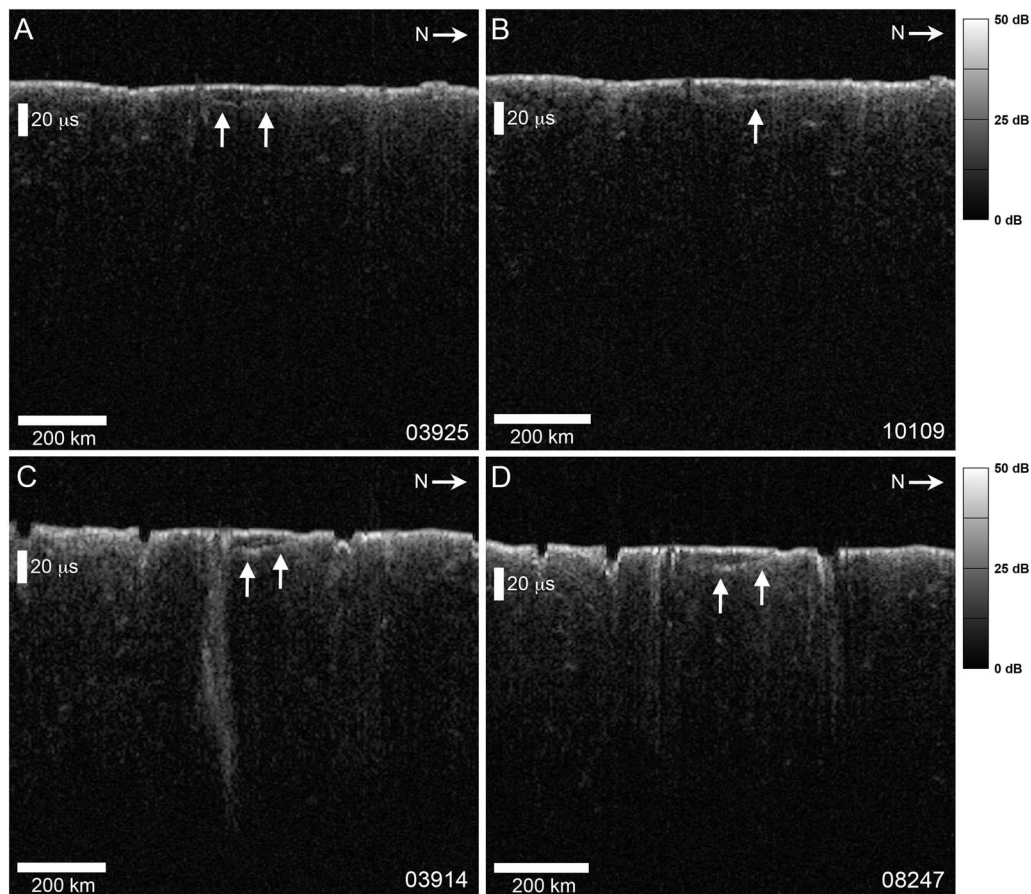


Figure 2. Radargrams showing MARSIS SS3 data for orbit (a) 03925, band 2, (b) 10109, band 3, (c) 03914, band 2, and (d) 08247, band 2 where echoes are plotted in time delay versus position along the orbit. The subsurface echoes (white arrows) are offset in time delay from the surface echo and are interpreted to be nadir reflections from the interface between the HBP-EP deposits and the cratered terrain. They suggest that the cratered terrain is locally relatively featureless. Orbit track locations are shown in Figure 1. North is to the right in the radargrams.

Grima et al., 2009], and these interpretations have been confirmed by the Shallow Radar (SHARAD) instrument on the Mars Reconnaissance Orbiter, operating in a single frequency band centered at 20 MHz [*Phillips et al., 2008; Seu et al., 2007*].

Even before the MARSIS radar sounder began its subsurface exploration, Opportunity was surveying surface exposures of the hematite-rich deposits of Meridiani Planum [*Squyres et al., 2004*] thought to have formed by the circulation of groundwater [*Squyres and Knoll, 2005; Arvidson et al., 2005; Gendrin et al., 2005*]. However, the makeup of the deposits below those examined by the Opportunity rover remains largely a mystery. The SHARAD radar sounder which has partially or completely penetrated PLD, MFF, and other possibly ice-rich deposits, detects no subsurface reflectors in Meridiani Planum deposits despite the surface being very smooth at the instrument's frequency [*Putzig et al., 2014*]. We report the detection of subsurface reflectors in MARSIS sounder data deep within the deposits of Meridiani Planum. The electrical and physical properties of the Meridiani deposits are characterized in an effort to determine their origin.

2. Subsurface Reflectors in Meridiani Planum

Radargrams for MARSIS SS3 mode orbits (see supporting information Text S1) covering the HBP-EP deposits east of the Opportunity landing site show subsurface echoes offset in time delay from the surface returns (Figures 2 and 3). The subsurface echoes are interpreted to be nadir reflections from the interface between the HBP-EP deposits and the underlying cratered terrain or a relatively deep interface within the deposits. Surface clutter from off-nadir sources is minimal because Meridiani Planum is generally featureless in the areas where subsurface reflectors are detected. Relatively deep subsurface echoes in data from orbits

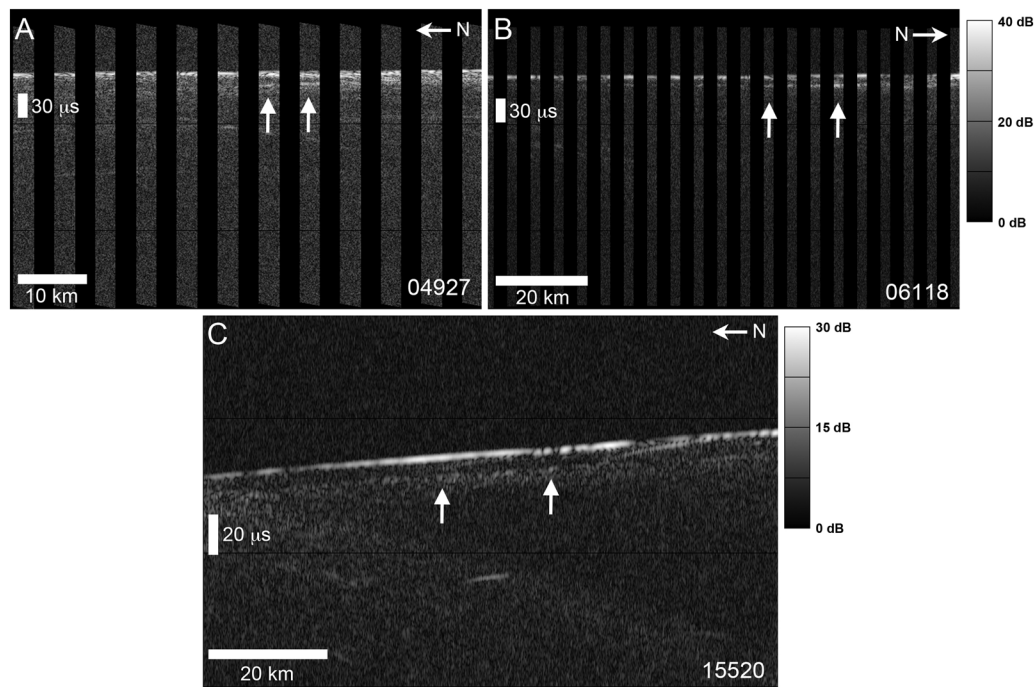


Figure 3. Radargrams showing MARSIS normal FM data for orbits (a) 04927, band 3 and (b) 06118, band 2, and MARSIS superframe FM data for orbit (c) 15520, band 2 where echoes are plotted in time delay versus position along the orbit. The subsurface echoes (white arrows) are offset in time delay from the surface echo and are interpreted to be nadir reflections from the interface between the HBP-EP deposits and the cratered terrain. Orbit track locations are shown in Figure 1. North is to the right in Figure 3b and to the left in 3a and 3c.

03925 and 10109 have maximum offsets in time delay from the surface returns of ~ 8 to $11 \mu\text{s}$ and are about 200 km east of the Opportunity landing site (Figures 2a and 2b), whereas subsurface echoes in orbits 03914 and 08247, located ~ 50 km farther east, show dipping subsurface echoes where HBP-EP deposits appear to thin locally to the north (Figures 2c and 2d). The maximum offsets in time delay from the surface return (~ 9 to $12 \mu\text{s}$) are comparable to those in the adjacent MARSIS SS3 orbits to the west (Figures 2a and 2b).

Subsurface echoes found in radargrams for MARSIS flash mode (FM) orbits (see the supporting information) (Figures 3a and 3b) with time delays of ~ 11 to $13 \mu\text{s}$ straddle those in the SS3 orbits (Figure 1). A MARSIS superframe FM orbit (see the supporting information) obtained in 2016 (15520) shows relatively deep subsurface echoes, offset a maximum of $\sim 11 \mu\text{s}$ in time delay from the surface return, located ~ 325 km northeast of the Opportunity landing site (Figure 1) and extending across much of the ~ 100 km length of the radargram (Figure 3c). The maximum offsets in time delay from the surface return are comparable to those in the normal FM orbits to the west (Figures 3a and 3b).

3. Electrical Properties of the Meridiani Planum Deposits

The electrical properties of the Meridiani Planum deposits can be evaluated using the MARSIS observations. The bulk real dielectric constant ϵ' , which is strongly modulated by bulk density, can be determined if the thickness of the HBP-EP deposits relative to the interface responsible for the subsurface echoes is known. Our interpretation is that the subsurface echoes are nadir reflections from the interface between the HBP-EP deposits and the underlying cratered terrain. Estimates of the maximum thickness of the HBP-EP deposits vary from ~ 600 to 900 m [Hynek *et al.*, 2002; Griffes *et al.*, 2007] and > 800 m [Edgett, 2005] based on elevation differences between the deposits and the adjacent cratered terrain.

In estimates of ϵ' for the PLD and MFF deposits, where MARSIS basal reflectors have equal or greater time delays, the thickness of these deposits has been determined from the agreement between the inferred depth of the basal interface and the projection of the surrounding surface [Plaut *et al.*, 2007; Watters *et al.*, 2007; Phillips *et al.*, 2008]. This approach is much more problematic for the Meridiani Planum deposits because of

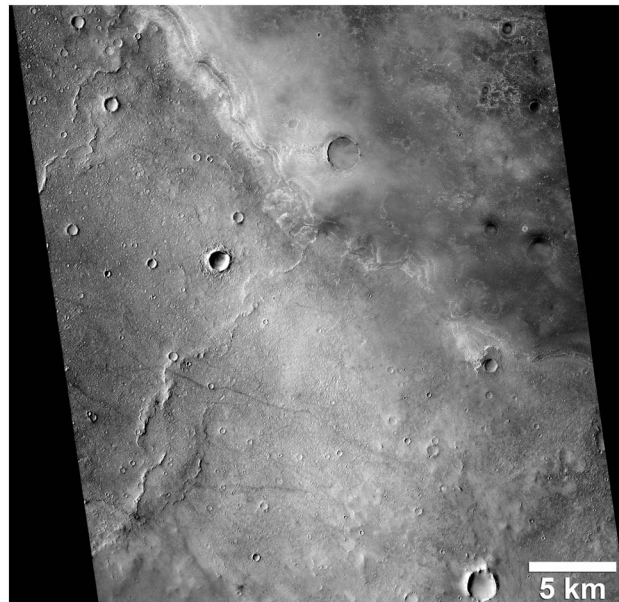


Figure 4. Floor of Miyamoto crater. CTX image showing an exposed portion of the floor of Miyamoto crater. Wrinkle ridges deform volcanic plains that underlie the layered HBP-EP deposits (upper right). CTX image frame J03_045773_1786_XI_01S007W.

the absence of a basal surface with a consistent elevation in the cratered highlands of Arabia Terra. One exception is the deposits partially filling the Miyamoto impact crater. Miyamoto crater is about 160 km in diameter and is located west of the Opportunity landing site (Figure 1). It is remarkable because layered Meridiani deposits bury its northern rim and half of its floor, and the exposed portion of the crater was a candidate Mars Science Laboratory landing site [Newsom *et al.*, 2010]. Of particular interest is the presence of volcanic plains on the exposed portion of Miyamoto's floor that likely extend beneath the HBP-EP [Newsom *et al.*, 2010; Edgett and Malin, 2008]. The identification of this unit as volcanic plains is supported by the presence of wrinkle ridges (Figure 4), contractional tectonic landforms common in deformed volcanic

sequences [Watters, 1988]. The presence of volcanic plains that are expected to form a roughly equipotential surface on the floor of Miyamoto crater provides a clear interface between the Meridiani deposits and the higher-density, likely basaltic sequence. Three MARSIS S53 mode, overlapping orbits, 04982, 05985, and 09347, cross Miyamoto crater near the center of the deposits (Figure 1). Radargrams for 05985 (Figure 5) and 04982 and 09347 (see supporting information Text S2 and Figures S1a and S1b) show subsurface reflectors we interpret to be from the interface between the HBP-EP deposits and the underlying basaltic plains. Topographic profiles obtained from Mars Orbiter Laser Altimeter (MOLA) gridded data along and bracketing the 05985, 04982, and 09347 ground tracks indicate a maximum thickness of the deposits of $\sim 400 \pm 11$ m. The observed time delays correspond to a ϵ' for the HBP-EP deposits in Miyamoto crater of 3.6 ± 0.6 (see supporting information Text S3). The curvature of the subsurface reflectors (Figure 5a and supporting

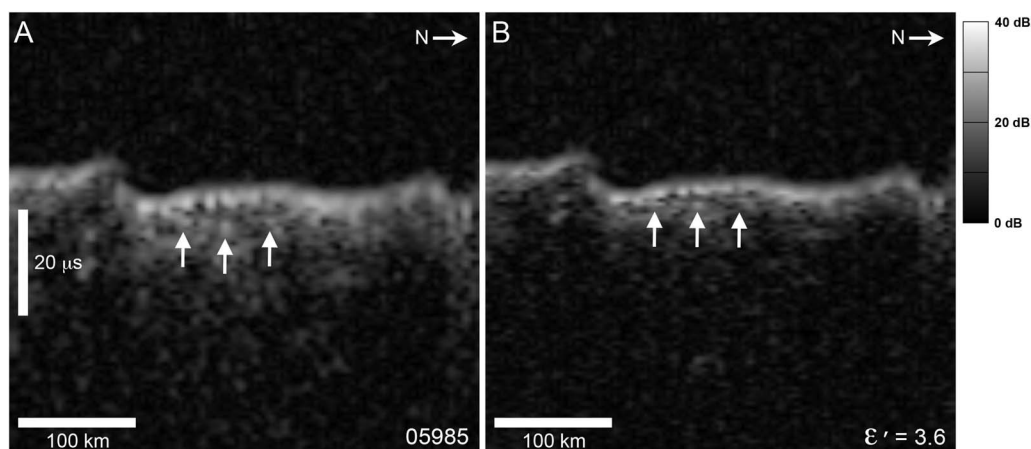


Figure 5. Radargram showing MARSIS S53 data for orbit 05985, band 1. (a) Echoes are plotted in time delay versus position along the orbit, and the discontinuous subsurface echoes (white arrows) are offset in time delay from the surface echo and are interpreted to be nadir reflections from the interface between the HBP deposits and volcanic plains on the floor of Miyamoto crater. (b) Radargram showing orbit 05985 converted from free space to depth using a dielectric constant $\epsilon' = 3.6$ for the HBP-EP deposits. The curved echo in Figure 5a appears flat and generally coincides with the projection of the volcanic plain in Miyamoto crater beneath the HBP-EP deposits. North is to the right in the radargrams. Orbit track location is shown in Figure 1.

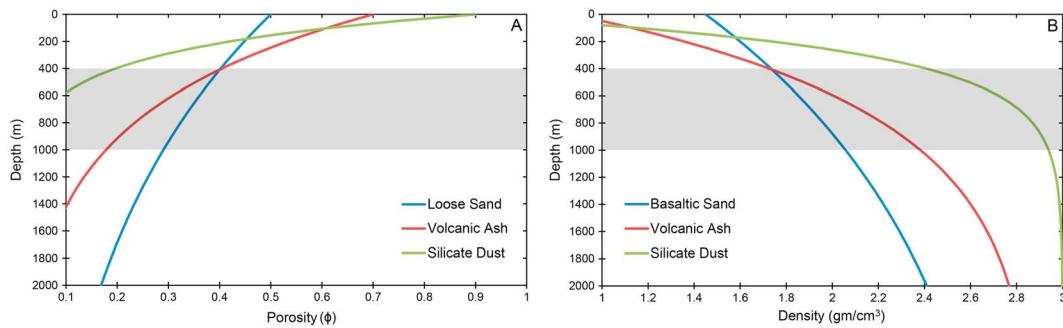


Figure 6. Compaction and density curves for three geologic materials: a loose basalt sand (blue), a volcanic ash (red), and a silicate dust (green). (a) The compaction model incorporates the compressibility of the materials and acceleration due to gravity of Mars (see supporting information equation (2)) and the material parameters). (b) Change in bulk density as a function of depth for the compacting materials. The bulk density increases with decreasing porosity (see supporting information equation (3)). The model assumes the density of the particles or grains ρ_p for basaltic sand and volcanic ash of 2.9 gm/cm^3 and 3.0 gm/cm^3 for silicate dust. The region of the plot in grey represents the approximate range in maximum depth of the Meridiani Planum deposits determined in this study.

information Figures S1a and S1b) is an artifact resulting from the time delay (free-space) representation of the data. Assigning a value of ϵ' of 3.6 converts the time delay representation to depth and flattens the subsurface echo, nearly matching a projection of the volcanic plain beneath the HBP-EP deposits in the crater (Figure 5b). Using this value of ϵ' , the thickness of HBP-EP deposits east of Miyamoto crater in the area of $\sim 0.5^\circ\text{W}$ – 2°W can be estimated. Assuming that $\epsilon' = 3.6$ and that the subsurface echoes are basal reflectors, the thickness of the HBP-EP deposits from seven SS3 and FM orbits (Figure 1), ranges from ~ 600 to 1000 m with a mean of ~ 840 m (number of measurements $n = 21$). This is in good agreement with published estimates of 600 to 900 m [Hynek *et al.*, 2002; Griffes *et al.*, 2007; Edgett, 2005].

4. Interpretation and Discussion

Although the composition of the exposed HBP surficial deposits has been established by the Opportunity rover, there is no consensus on the nature of underlying EP deposits. Suggested origins include paleopolar dust deposits [Schultz and Lutz, 1988], eolian sediments [Scott and Tanaka, 1986], and friable volcanic ash deposits Hynek *et al.*, 2002, 2003]. Cliff-forming outcrops and the lack of boulders and high thermal inertia surfaces in these light toned deposits suggest that they are weakly indurated [see Grotzinger and Milliken, 2012]. The electrical properties inferred from the sounder data allow discrimination between some of these possible explanations.

A real dielectric constant of ~ 3.6 is consistent with a low bulk density over much of the thickness of the EP deposit or a very high fraction of water ice. Pore-filling and porous water ice have been proposed to account for low values of ϵ' in some middle- to low-latitude deposits [Plaut *et al.*, 2009; Bramson *et al.*, 2015; Stuurman *et al.*, 2016], but the deposits of Meridiani Planum are distinctly different. The fact that no subsurface reflectors have been detected in SHARAD sounder data [Putzig *et al.*, 2014] distinguishes the HBP-EP from other deposits with relatively low bulk dielectric constants that the SHARAD radar sounder successfully penetrates.

The HBP-EP appears to have formed in a unique physiographic and hydrologic setting where ancient, prolonged groundwater upwelling occurred in a low-lying region [Andrews-Hanna *et al.*, 2007]. Such an environment may have been an ideal sediment trap [Grotzinger and Milliken, 2012], allowing deposition of a thick sequence of eolian sands. Subsequent sustained evaporation likely left these deposits dry. This is supported by improved spatial resolution epithermal neutron data from the Mars Odyssey Neutron Spectrometer that indicate no enrichment of subsurface hydrogen over much of Meridiani Planum [Wilson *et al.*, 2017]. Assuming that the EP deposits are ice poor, we consider three possibilities; they are composed dominantly of a thick sequence of (1) eolian basaltic sand, (2) volcanic ash, or (3) silicate dust.

A critically important consideration is the degree to which a thick, porous sequence of such deposits will compact with depth. Compaction results in a decrease in the porosity and an increase in bulk density. Compaction models that estimate porosity as a function of depth and incorporate the acceleration due to gravity of Mars, (see supporting information Text S4 for an explanation of the model and the physical parameters for basaltic sand, volcanic ash, and silicate dust) indicate that basaltic sand experiences the least

reduction in porosity with depth (a reduction from 50% to ~40% at 400 m depth compared to a reduction from 70% to ~40% for volcanic ash and from 90% to ~20% for lunar-like dust) (Figure 6a). Model results show that a loose, basaltic sand assumed to have an approximate porosity of 50% at the surface and a corresponding density of $\sim 1.43 \text{ gm/cm}^3$ will increase in density to $\sim 1.74 \text{ gm/cm}^3$ at a depth of 400 m (Figure 6b). Volcanic ash with a decrease in ϕ from 70% to ~40% at 400 m depth also increases to a density of $\sim 1.73 \text{ gm/cm}^3$ and silicate dust with a decrease in ϕ from 90% to ~20% at 400 m depth increases to a density of $\sim 2.41 \text{ gm/cm}^3$. At a depth of 1000 m, however, the density of a compacting basaltic sand increases to a density of only $\sim 2.06 \text{ gm/cm}^3$, while a compacting volcanic ash reaches a density of $\sim 2.38 \text{ gm/cm}^3$ (Figure 6b). The real dielectric constant is a function of density and for geologic materials is approximated by $\epsilon' = 1.96^{\rho_b}$, where ρ_b is the bulk density [Ulaby *et al.*, 1988]. The near-surface dielectric constant for ρ_b of 1.43 gm/cm^3 is ~ 2.65 , in the midrange of experimentally derived values for dry, loose sand and coarse sand/small pebble materials (~ 2.1 to 3.6) [Williams and Greeley, 2004].

A compacting deposit does not have a uniform density, so the two-way travel time is related to the integral of the effective speed of light over the unit depth. Thus, the compacted deposit will have an effective real dielectric constant ϵ' that relates the observed two-way travel time to the change in the index of refraction with depth (see supporting information). Model results indicate that a 400 m thick unit of basaltic sand has an apparent $\epsilon' \cong 3.0$, and a 1000 m thick unit has an apparent $\epsilon' \cong 3.3$ (see supporting information Figure S5). A bulk value of $\epsilon' \sim 3.6 \pm 0.6$ is thus consistent with the HBP-EP deposit consisting largely of dry basaltic sand that forms a weakly indurated sandstone.

MARSIS radar sounder data and our modeling indicate that the relatively low derived dielectric constant of the Meridiani Planum deposits ($\sim 3.6 \pm 0.6$) is consistent with a thick, low-density sequence of porous, basaltic sand (density at the surface and at 1 km depth of ~ 1.43 and $\sim 2.06 \text{ gm/cm}^3$, respectively). Pore-filling water ice is therefore not necessary to explain the low dielectric constant of the Meridiani Planum deposits. These results show that materials with relatively low real dielectric constant values, similar to those estimated for some nonpolar deposits, may be realized with a high-porosity matrix and a low to zero fraction of pore-filling water ice. The relatively low acceleration due to gravity and the cold, dry climate that has dominated Mars for billions of years may have allowed large, widely distributed eolian sand deposits to remain porous and only weakly indurated.

Acknowledgments

MARSIS is managed by the Agenzia Spaziale Italiana (ASI) and the National Aeronautics and Space Administration (NASA). The Mars Express mission is managed and operated by the European Space Agency. The full MARSIS radargrams used in this study are available on the Smithsonian's National Air and Space Museum Data Repository website (<https://airand-space.si.edu/research/data-repository>).

References

- Andrews-Hanna, J. C., R. J. Phillips, and M. T. Zuber (2007), Meridiani Planum and the global hydrology of Mars, *Nature*, *446*, 163–166.
- Arvidson, R. E., et al. (2003), Mantled and exhumed terrains in Terra Meridiani, Mars, *J. Geophys. Res.*, *108*(E12), 8073, doi:10.1029/2002JE001982.
- Arvidson, R. E., F. Poulet, J.-P. Bibring, M. Wolff, A. Gendrin, R. V. Morris, J. J. Freeman, Y. Langevin, N. Mangold, and G. Bellucci (2005), Spectral reflectance and morphologic correlations in eastern Terra Meridiani, Mars, *Science*, *307*, 1591–1594.
- Bramson, A. M., S. Byrne, N. E. Putzig, S. Sutton, J. J. Plaut, T. C. Brothers, and J. W. Holt (2015), Widespread excess ice in Arcadia Planitia, Mars, *Geophys. Res. Lett.*, *42*, 6566–6574, doi:10.1002/2015GL064844.
- Carter, L. M., et al. (2009), Shallow radar (SHARAD) sounding observations of the Medusae Fossae Formation, Mars, *Icarus*, *199*, 295–302.
- Christensen, P. R., et al. (2000), Detection of crystalline hematite mineralization on Mars by the thermal emission spectrometer: Evidence for near-surface water, *J. Geophys. Res.*, *105*, 9623–9642, doi:10.1029/1999JE001093.
- Edgett, K. S. (2005), The sedimentary rocks of sinus Meridiani: Five key observations from data acquired by the Mars global surveyor and Mars odyssey orbiters, *Intern. J. Mars Sci. Exploration*, *1*, 5–58.
- Edgett, K. S., and M. C. Malin (2008), MRO context camera (CTX) investigation primary mission results (abstract), *Eos*, *89*, P31D-04.
- Gendrin, A., et al. (2005), Sulfates in Martian layered terrains: The OMEGA/Mars express view, *Science*, *307*, 1587–1591.
- Griffes, J. L., R. E. Arvidson, F. Poulet, and A. Gendrin (2007), Geologic and spectral mapping of etched terrain deposits in northern Meridiani Planum, *J. Geophys. Res.*, *112*, E08S09, doi:10.1029/2006JE002811.
- Grima, C., W. Kofman, J. Mouginot, R. J. Phillips, A. Hérique, D. Biccari, R. Seu, and M. Cutigni (2009), North polar deposits on Mars: Extreme purity of the water ice, *Geophys. Res. Lett.*, *36*, L03203, doi:10.1029/2008GL036326.
- Grotzinger, J. P., and R. E. Milliken (2012), *The Sedimentary Rock Record of Mars: Distribution, Origins, and Global Stratigraphy*, SEPM Special Publication, vol. 102, SEPM (Society for Sedimentary Geology). [Available at <https://www.crossref.org/iPage?doi=10.2110%2Fpec.12.102.0001>].
- Hynek, B. M., and G. Di Achille (2017), *Geologic Map of Meridiani Planum, Mars, U.S. Geological Survey Scientific Investigations Map 3356*, U.S. Geol. Surv., doi:10.3133/sim3356. [Available at <https://pubs.er.usgs.gov/publication/sim3356>].
- Hynek, B. M., R. E. Arvidson, and R. J. Phillips (2002), Geologic setting and origin of Terra Meridiani hematite deposit on Mars, *J. Geophys. Res.*, *107*(E10), 5088, doi:10.1029/2002JE001891.
- Hynek, B. M., R. J. Phillips, and R. E. Arvidson (2003), Explosive volcanism in the Tharsis region: Global evidence in the Martian geologic record, *J. Geophys. Res.*, *108*(E9), 5111, doi:10.1029/2003JE002062.
- Jordan, R., et al. (2009), The Mars express MARSIS sounder instrument, *Planet. Space Sci.*, *57*, 1975–1986.
- Morgan, G. A., B. A. Campbell, L. M. Carter, and J. J. Plaut (2015), Evidence for the episodic erosion of the Medusae Fossae Formation preserved within the youngest volcanic province on Mars, *Geophys. Res. Lett.*, *42*, 7336–7342, doi:10.1002/2015GL065017.

- Newsom, H. E., et al. (2010), Inverted channel deposits on the floor of Miyamoto crater, Mars, *Icarus*, 205, 64–72.
- Orosei, R., et al. (2015), Mars advanced radar for subsurface and ionospheric sounding (MARSIS) after nine years of operation: A summary, *Planet. Space Sci.*, 112, 98–114.
- Picardi, G., et al. (2005), Radar soundings of the subsurface of Mars, *Science*, 310, 1925–1928.
- Phillips, R. J., et al. (2008), Mars north polar deposits: Stratigraphy, Age, and Geodynamical Response, *Science*, 320, 1182–1185.
- Plaut, J. J., et al. (2007), Subsurface radar sounding of the south polar layered deposits of Mars, *Science*, 316, 92–95.
- Plaut, J. J., A. Safaeinili, J. W. Holt, R. J. Phillips, J. W. Head III, R. Seu, N. E. Putzig, and A. Frigeri (2009), Radar evidence for ice in lobate debris aprons in the mid-northern latitudes of Mars, *Geophys. Res. Lett.*, 36, L02203, doi:10.1029/2008GL036379.
- Putzig, N. E., R. J. Phillips, B. A. Campbell, M. T. Mellon, J. W. Holt, and T. C. Brothers (2014), SHARAD soundings and surface roughness at past, present, and proposed landing sites on Mars: Reflections at Phoenix may be attributable to deep ground ice, *J. Geophys. Res. Planets*, 119, 1936–1949, doi:10.1002/2014JE004646.
- Seu, R., et al. (2007), SHARAD sounding radar on the Mars Reconnaissance Orbiter, *J. Geophys. Res.*, 112, E05S05, doi:10.1029/2006JE002475.
- Schultz, P. H., and A. B. Lutz (1988), Polar wandering on Mars, *Icarus*, 73, 91–141.
- Scott, D. H., and K. L. Tanaka (1986), Geologic map of the western equatorial region of Mars, *U.S. Geol. Surv. Misc. Invest. Ser. Map, I-1802-A*.
- Squyres, S. W., and A. H. Knoll (2005), *Sedimentary Geology at Meridiani Planum, Mars*, Elsevier, New York.
- Squyres, S. W., et al. (2004), In situ evidence for an ancient aqueous environment at Meridiani Planum, *Science*, 306, 1709–1714.
- Stuurman, C. M., G. Osinski, J. W. Holt, J. S. Levy, T. C. Brothers, M. Kerrigan, and B. A. Campbell (2016), SHARAD detection and characterization of subsurface water ice deposits in utopia Planitia, Mars, *Geophys. Res. Lett.*, 43, 9484–9491, doi:10.1002/2016GL070138.
- Ulaby, F. T., et al. (1988), *Microwave Dielectric Spectrum of Rocks*, Univ. of Michigan, Ann Arbor, Mich.
- Watters, T. R. (1988), Wrinkle ridge assemblages on the terrestrial planets, *J. Geophys. Res.*, 93, 10,236–10,254, doi:10.1029/JB093iB09p10236.
- Watters, T. R., et al. (2007), Radar sounding of the Medusae Fossae Formation Mars: Equatorial ice or dry, low-density deposits?, *Science*, 318, 1125–1128.
- Williams, K. K., and R. Greeley (2004), Measurements of dielectric loss factors due to a Martian dust analog, *J. Geophys. Res.*, 109, E10006, doi:10.1029/2002JE001957.
- Wilson, J. T., et al. (2017), Equatorial locations of water on Mars: Improved resolution maps based on Mars Odyssey Neutron Spectrometer data, *Icarus*, 299, 148–160.